Study of the Ferrofluid Drying Process for Morphological and Nanostructutal Characterization

L. F. Gamarra[a,b], G. E. S. Brito[b], W. M. Pontuschka[b], J. B. Mamani[b], C. A. Moreira-Filho[a,c], and E. Amaro Jr.[a,d]
[a] Instituto Israelita de Ensino e Pesquisa Albert Einstein, IIEP, São Paulo, 05651-901, Brazil
[b] Instituto de Física, Universidade de São Paulo, São Paulo, Brazil
[c] Departamento de Imunologia, Instituto de Ciências Biomédicas, Universidade de São Paulo, São Paulo, Brazil and
[d] Instituto de Radiologia InRad, Faculdade de Medicina, Universidade de São Paulo, São Paulo, Brazil

Received on 2 October, 2007

A drying method suitable for the study of the morphological and structural properties of colloidal magnetic systems, including a contrast agent used in Magnetic Resonance Imaging (MRI) is described. We tested three alternative ferrofluid drying methods: drying at 70 °C in nitrogen atmosphere; drying in air at 70 °C; and drying by liophylization using an MRI marker in the form of a colloidal suspension (Endorem^{TM} - Guebert). X-ray diffraction (XRD), and transmission electron microscopy (TEM) were applied to each characterization method. The XRD allowed the observation of the possible physical-chemical changes of the stabilizers and also Fe_3O_4 present in the system. The morphology and nanoparticles size distribution was analyzed by TEM. Among the drying methods examined in this study, the liophylization has shown to be the more adequate one for the nanoparticles (Fe_3O_4) morphological study and nanostructural characterization, because the structure of the nanoparticles was maintained the same as in the suspension. The drying procedures performed at 70 °C in the atmospheres of nitrogen and air let to the coalescence and growth of the nanoparticles, as well as some degradation has been noticed in some of the stabilizers.

Keywords: Lyophilization; Ferrofluid; Endorem; Magnetic nanoparticles

I. INTRODUCTION

Magnetic fluids or ferrofluids are concentrated and stable colloidal suspensions usually composed of a dispersed phase of iron oxide magnetic nanoparticles such as the ferrites. These nanoparticles usually consist of magnetic single-domain phases which are dispersed into an organic (alcohols and alkil-benzene) or inorganic (water) liquid phase. The ferrofluid has the fluidity of a homogeneous solution of high magnetic susceptibility [1–4].

A ferrofluid is said to be biocompatible when it is stable in physiological conditions, it has a neutral pH and 0.9 % of salinity [5, 6]. This is achieved by covering the nanoparticles by a biocompatible molecular layer in order to prevent the formation of large clusters, modifications in the original structure and biodegeneration, when exposed to the biological systems [7, 8].

The magnetic nanoparticles are an alternative class of contrast agents for magnetic resonance imaging (MRI) since they modulate proton behavior in different tissues [9–12], allowing access to structural information of the living organ under study based on a biological distribution of the contrast. In order to produce a distinct contrast in the MR images, the main property of an ferrofluid particle is the ability to modify the local magnetic environment: the magnetic susceptibility effect. The magnetic susceptibility of a solution is associated with the nanoparticle size [13]. However, the techniques used to evaluate the morphology of the nanoparticles are still in development stage and they present advantages and shortcomings [14].

TEM images of the nanoparticles do not represent their actual arrangement when in suspension since the microstructure may be severely distorted on drying [15].

The objective of the present work is to propose an adequate drying method for ferrofluids which is necessary for their morphological and structural characterization, immediately after synthesis. This information is fundamental to maintain a more efficient control over their physical-chemical properties, preventing against the coalescence of the nanoparticles, and preserving their morphology and structure without decomposition of additives [13].

We used a commercially available component, Endorem^{TM} [16] to which we applied three drying methods: at 70^{o}C in nitrogen and air in atmosphere and by liophylization.

XRD methods were used to find evidence of the probable iron oxide phase and to detect possible physical-chemical changes at the stabilizers. The morphological and the nanoparticles distribution analyses were carried out by using TEM and compared to the values provided by the manufacturer [16].

II. EXPERIMENTAL PROCEDURE

Endorem^{TM} (Endorem^{TM}-Guebert, earlier trade name AMI-25, Laboratoire Guebert, France [16]) is a biocompatible ferrofluid used as an MRI marker. It consisted of a suspension of 126.500 mg of Fe_3O_4 superparamagnetic nanoparticles contained in 8 ml of water. The nanoparticles of average diameter of 10 nm size are coated with low-weight dextran (79 kDa) [17] of hydrodynamic diameters between $80 - 150\,nm$. In addition to water, the solvent composition consisted of 60.800 mg of dextran, 2.714 mg of citric acid, and 490.400 mg of β-D-mannitol ($C_6H_{14}O_6$).

The drying procedure in the nitrogen atmosphere at 70 °C was performed during 30 min in a stove with accurate temperature control. Drying in air at 70 °C was carried out with the same conditions as of the preceding method, but in the

ambient air atmosphere. The drying by liophylization, also known as freeze drying process, was performed at -5 °C on a $10^{-3}\,mmHg$ vacuum chamber.

The crystalline phase and the structure of the nanoparticles of the powders obtained after drying were characterized by XRD at the sweeping interval of 10 at 70 °C (2θ) with steps of 0.05° for each $10\,s$, using a beam of $Cu - K_\alpha(1.5418\ \AA)$ and Si monochromator. To study the morphology of the nanoparticles samples of each dried powder were dispersed over copper grids covered with collodium and carbon [18] and then they were examined in a Leo 906E (Zeiss) TEM at $80\,Kv$.

The size poly-dispersity of the nanoparticles was analyzed from the TEM digitized micrographs using an image analysis software (Java version of Image J v 1.33u [19]). Mean diameters were obtained by fitting the experimental data with a lognormal distribution function, as suggested by O'Grady and Bradbury [20],

$$f(D_P) = \frac{1}{\sqrt{2\pi}\omega_P D_P} exp(-\frac{(ln\,D_P - ln\,D_P^0)^2}{2\omega_P^2}), \qquad (1)$$

with mean diameter $< D_P >= D_P^0 exp(\omega_P^2/2)$ and ω_P as the standard deviation around $ln\,D_P^2$. The standard deviation of the mean diameter σ_P is

$$\sigma_P = D_P^0[exp(2\omega_P^2) - exp(\omega_P^2)]^{1/2}\ . \qquad (2)$$

III. RESULTS AND DISCUSSIONS

For a better understanding of the physical-chemical behavior of the ferrofluid during the drying process, we first applied a XRD analysis of the modifications occurred in the stabilizers. The observation of the presence of Fe_3O_4, as well as the effect of the air atmosphere and its physical-chemical influence on the structure of the nanoparticles were also evaluated. The alterations in the XRD peaks were observed in each drying method, as shown in Figs. 1, 2 and 3, respectively. It should be mentioned that XRD is not sensitive to quantities smaller than 5 % in volume, which is the case of the citric acid, a substance not detectable by this technique.

The powder diffractogram of the drying at 70 °C in nitrogen atmosphere (Fig. 1) shows a reduction of the stabilizers. This can be due to the breakdown catalytic effect of the high surface energy of the nanometric particles, which makes it more vulnerable to degradations or phase change. This drying process has also favored all the coalescence mechanisms. XRD showed the presence of the β-D-mannitol phase (orthorhombic structure), providing evidence of phase change. The data were compared with those of the International Center for Diffraction Data (ICDD), file #22 – 1797. The diffractogram shows evidence of Fe_3O_4, peaks of low intensity, as already expected.

The powder diffractogram of the sample dried at 70 °C in air (Fig. 2) has shown little decomposition of stabilizers, in a situation where all mechanisms leading to the particle coalescence and growth are operating. The XRD analysis showed evidence of presence of two phases of D-mannitol (α-D-Mannitol and β-D-mannitol), these data were compared with ICDD files #22 – 1797 and #22 – 1793, respectively. We observed traces of Fe_3O_4, peaks of low intensity, as in similar observations made in the previous drying process.

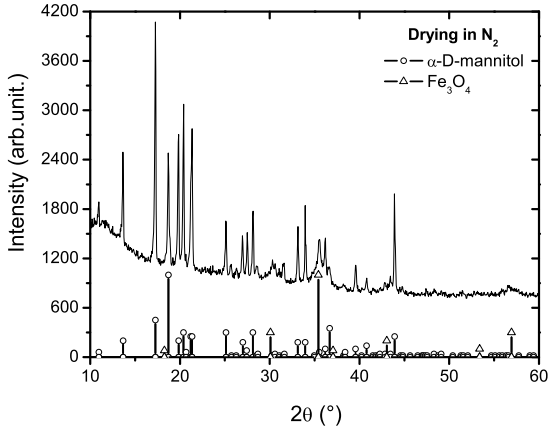

FIG. 1: Diffractogram of the powder, dried at 70 °C in N_2 atmosphere, showing evidence of α-D-mannitol phase, representing possible reduction of the stabilizers.

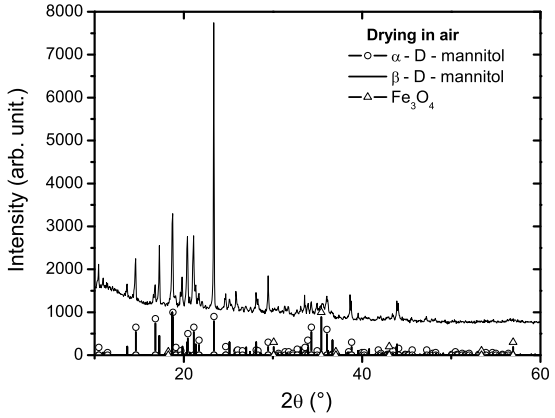

FIG. 2: Diffractogram of the powder dried at 70 °C in air showing the evidence of both phases of D-mannitol (α-D-mannitol and β-D-mannitol).

The diffractogram of the powder obtained after liophylization of the colloidal suspension (Fig. 3), showed peaks attributed only to β-D-mannitol, and no change in the stabilizers was noticed. The lyophilized powder preserved the ferrofluids, the capillary tensions are eliminated and the condensation rate is negligible due to its endothermic character. It was possible to freeze the ferrofluid structure without the interference of any physical-chemical changes. Traces of Fe_3O_4 were ob-

served as in the previous cases.

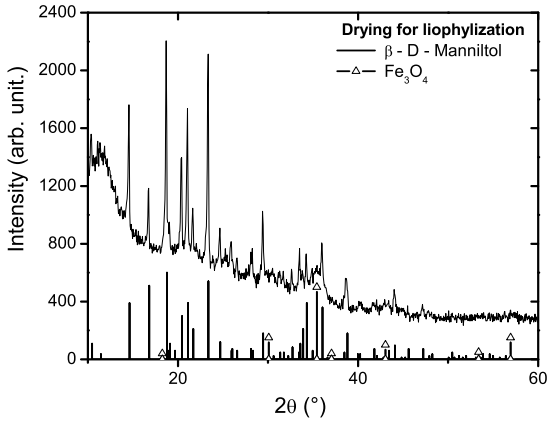

FIG. 3: Diffractogram of the powder dried by liophylization. Evidence of the stabilizer preservation and the presence of the β-D-mannitol peaks are shown.

In all of the three drying methods of this study the weak and broad profiles of Fe_3O_4 could be observed, as expected for nanoparticle powder. Peaks of the stabilizers are seen superimposed to these peaks.

The morphology of the particles and their distribution was analyzed by TEM. Figs. 4 and 5 show the micrographs of the atmospheres of nitrogen and air, respectively. It can be noted that the average diameter of the nanoparticles is about $20\,nm$ in N_2 and $15\,nm$ in air. These values are higher than those of $10\,nm$ reported in reference [16]. The increased diameters can be explained by the coalescence phenomenon and growth of the nanoparticles, governed by oxolation reaction.

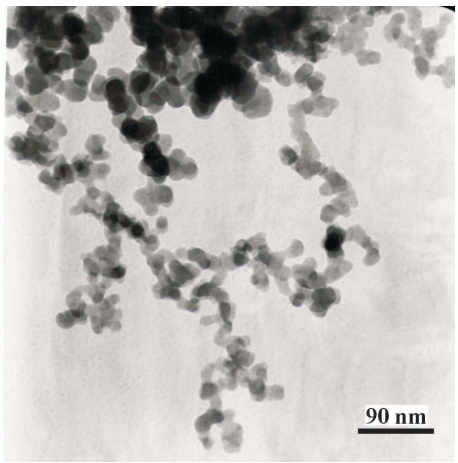

FIG. 4: Micrograph of the commercial ferrofluid powder, after drying at 70°C in nitrogen atmosphere.

In the micrograph of the lyophilized powder (Fig. 6), the average diameter of the nanoparticles is 10 nm, corresponding to the value informed by the manufacturer. The histogram

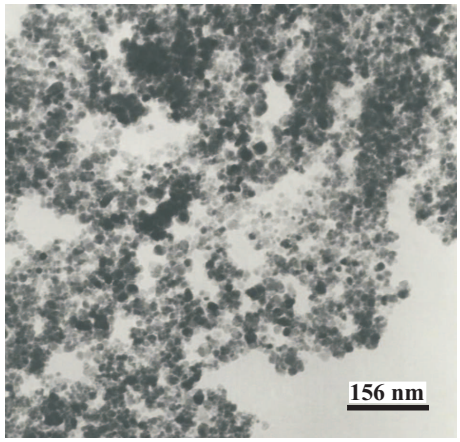

FIG. 5: Micrograph of the commercial ferrofluid powder, after drying at 70°C in air.

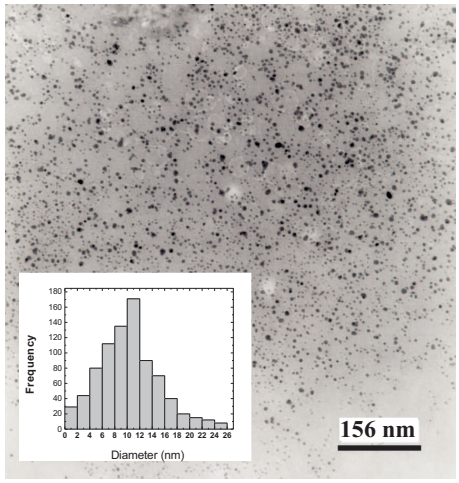

FIG. 6: Micrograph of the commercial ferrofluid powder after drying by liophylization. The inset is a histogram of the distribution of nanoparticles sizes, after lyophilization, obtained by TEM, using the approximation of a log-normal distribution of average diameter $< D_P >= 10.0\,nm$ and standard deviation $\sigma_P = 0.3\,nm$.

shown in the inset of Fig. 6 was obtained from the micrograph (Fig. 6) using the analysis processing program Image J 1.33u [19]. Is shown in the Inset of Fig. 6 the poly dispersity of the nanoparticles size and their distribution, adjusted to a log-normal distribution [20] with average diameter $< D_P >= 10.0\,nm$ and standard deviation $\sigma = 0.3\,nm$ over a total number of more than 800 particles. The program could not be applied to Figs. 4 and 5 micrographs because of the lack of representativeness of the particles morphology.

IV. CONCLUSION

It was shown that the drying method by liophylization produced the best results to obtain the ferrofluid solute in powder form without the physical-chemical changes that could interfere in the nanoparticle analysis. The other drying methods

(drying at 70 °C in nitrogen and in air) led to the coalescence and growth of the nanoparticles.

The XRD has provided evidence for the presence of peaks corresponding to β-D-mannitol stabilizers in the lyophilized sample, with no change of stabilizers phase, in contrast to what was observed in the other drying methods.

Among the three drying methods of this study, the liophylization method has proved to be the more adequate for the colloidal magnetic systems since it preserves the structure and morphology of the nanoparticles as they are in the suspension form. We have used this drying method in recent investigations [21, 22].

Acknowledgments

This work was supported by Instituto de Ensino e Pesquisa Albert Einstein, CNPq and Instituto do Milênio de Fluidos Complexos.

[1] W. Schutt, C. Gruttner, U. Hafeli, M. Zborowski, J. Teller, H. Putzar, and C. Schumichen, Hybridoma **16**, 109 (1997).
[2] X. Batlle and A. Labarta, J. Phys. D: Appl. Phys. **35**, R15 (2002).
[3] J. Frenkel and J. Dorman, Nature **126**, 274 (1930).
[4] C. P. Bean and J. D. Livingston, J. Appl. Phys. **30**, 120 (1959).
[5] Cecilia Albornoz and E. Jacobo Silvia, J. Magn. and Magn. Mater. **305**, 12 (2006).
[6] R. Langer, Science **249**, 1527 (1990).
[7] U. Hafeli, W. Schutt, J. Teller, and M. Zborowski, Scientific and Clinical Applications of Magnetic Carriers. New York, Plenum (1997).
[8] B. Denizot, G. Tanguy, F. Hindre, E. Rump, J. J. Lejeune, and P. Jallet, Journal Colloid Interface Sci. **209**, 66 (1999).
[9] T. Bach-Gansmo, Acta Radiol. [Suppl] **387**, 1 (1993).
[10] P. Reimer and B. Tombach, Eur. Radiol. **8**, 1198 (1998).
[11] S. Rubnic, A. R. Padhani, P. B. Revell, and J. E. Husband, Am. J. Roentgenol **173**, 173 (1999).
[12] Y. X. Ang, S. M. Hussain, and G. P. Krestin, Eur. Radiol. **11**, 2319 (2001).
[13] C. W. Jung and P. Jacobs, Magn. Reson. Imaging **13**, 661 (1995).
[14] Akito Sasaki, The rigaku journal **22**, 31 (2005).
[15] K. Butter, P. H. H. Bomans, P. M. Frederik, G. J. Vroege, and A. P. Philipse, Nature Materials **2**, 88 (2003).
[16] www.guerbt.com.br/portugues/endorem.htm
[17] M. Laniado, A. Chachuat, Vertraglichkeitsprofil von ENDOREM, Radiologe **35**, (Suppl. e), S266 (1995).
[18] B. M. Lacava, R. B. Azevedo, L. P. Silva, Z. G. M. Lacava, K. Skeff Neto, N. Buske, A. F. Bakuzis, and P. C. Morais, Appl. Phys. Lett. **77**, 1876 (2000).
[19] W. Rasvand, Image processing and analysis in Java URL http://rsb.info.nig.gov/ij 06-10-2004.
[20] K. O'Grady and A. Bradbury, J. Magn. and Magn. Mater. **39**, 91 (1983).
[21] L. F. Gamarra, G. E. S. Brito, W. M. Pontuschka, E. Amaro, A. H. C. Parma, and G. F. Goya, J. Magn. and Magn. Mater. **289**, 439 (2005).
[22] A. D. Arelaro, A. L. Brandi, E. Lima Jr., L. F. Gamarra, G. E. S. Brito, W. M. Pontuschka, and G. F. Goya, J. Appl. Phys. **97**, 10J316 (2005).